研究計畫中英文摘要：

（一） 計畫中文摘要:

背　景：心房顫動及心臟衰竭是兩種非常常見的心血管疾病。許多臨床及動物實驗皆顯示持續心房顫動會去除心室填充時的心房助力、引發心肌病變而導致心臟衰竭。另一方面，心臟衰竭時，纖維化或細胞凋零所致心房擴大，以及心房之結構與電氣再塑也有助於心房顫動的引發與維持。以抗心律不整藥物治療心房顫動已經證實可以改善心衰竭，同時像抑制腎素/血清張力素系統及 statin 類抗發炎等治療心衰竭及缺血性心臟病之非心律不整藥物最近已成為控制心房顫動另一策略。然而其確切的機轉仍然不明。在人體試驗中，血清張力素第二型受體阻斷(ARB)治療已顯示可降低心衰竭病患心房顫動的發生率，而於心臟手術前接受 statin 治療有助於減少術後心房顫動的發生。在動物實驗中已發現 ARB 和 statin 在狗的慢性心房顫動模型可減輕心房再塑。然而它們對心衰竭引起之心房再塑的作用仍不清楚。因此，在我們第一年的研究中，我們嘗試評估心臟衰竭後心房之組織病理特性。

方　法：我們在非接觸式立體定位系統偵測下，6 隻正常成狗及 6 隻心臟衰竭成狗(右心室快速電刺激每分鐘 240 跳持續 4-6 週)分別將心臟取出，再接上蘭根道夫(Langendorff)模式，之後接受不同部位電刺激，記錄右心房組織電位變化，並藉由立體定位標誌電位較高及電位較低之心房組織，電生理檢查完成後將心臟自狗取出，進行組織採樣。最後使用組織顯微鏡檢、定量免疫標定與西方墨點標誌分析對不同細胞標記的分布與表現進行分析。

結　果：心電生理特性中心臟衰竭狗與正常狗相近，但心房顫動引發的機率及維持心房顫動的時間皆較正常狗來得高。右心房組織不論是連結素 43 或者是 type I collagen，在正常狗或是心衰竭狗數值相當。但是在左心房組織則有不同的表現，關於 type I collagen 數值在正常狗或是心衰竭狗數值相當，但是心臟衰竭狗之連結素 43 明顯要低於正常狗。

結　論：在心臟衰竭狗之心房電生理特性明顯比正常狗容易產生心房顫動，同時連結素 43 在心臟衰竭狗之左心房明顯要低於正常狗，此等特質可能與左心房較易引發心房顫動有關。

關鍵詞: 血管張力素、心房顫動、再塑、心衰竭、statin

（二） 計畫英文摘要:

Background：Atrial fibrillation (AF) and congestive heart failure (CHF) are two very common cardiovascular disorders. Clinical and experimental studies have demonstrated that sustained AF abolishes atrial kick for ventricular filling, induces cardiomyopathy, and results in CHF. On the other hand, during CHF, atrial dilatation with fibrosis or apoptosis occurs, and both structural and electrical remodeling in atria may contribute to the initiation and maintenance of AF. While antiarrhythmic treatment for AF has been proved to improve CHF, non-antiarrhythmic therapy for CHF and ischemic heart disease, such as inhibition of renin-angiotensin system and anti-inflammation with statins, has recently become one alternative strategy for AF control. However, the underlying mechanisms are not detailed. In human studies, angiotensin II receptor blocker (ARB) treatment have been shown to be associated with lower AF incidence in CHF patients, and statin treatment before cardiac surgery contributes to the reduction of postoperative AF occurrence. In animal studies, ARB and statin has been found to attenuate atrial remodeling in canine chronic AF models. However, their role in CHF mediated atrial remodeling remains unclear. Therefore, in our study, we tried to evaluate the effects of non-antiarrhythmic treatment with irbesartan and artovastatin in the canine CHF models. In first year, we will evaluate the atrial pathologic change after CHF.

Methods：Under the guidance of noncontact mapping system, 6 adult normal and HF dogs (a rapid ventricular pacing of 240 bpm for 4-6 weeks) received electric stimulation from different sites in different coupling intervals. AF was induced from multiple pacing sites and the duration of induced AF was determined. After noncontact mapping, 8 to 10 pieces of atrial tissues were sampled from different sites of RA and LA for analysis of gap junctions, including connexin43 (Cx43) type I collagen levels..

Results：In the electrophysiological properties, the HF dogs had similar properties to the control dogs in four different atrial sites. However, the HF dogs had a higher AF inducibility and longer duration of AF paroxysms than normal dogs. In the Western blotting analysis of total Cx43 protein and type I collagen levels in the RA and LA of the control and CHF dogs, the type I collagen levels in the RA and LA were similar between the control and CHF dogs. However, in the RA, the Cx43 levels were similar among normal and CHF dogs but in the LA, the Cx43 levels were significantly declined in CHF dogs than in normal dogs.

Conclusions: In dogs with 4 to 5 weeks of rapid ventricular pacing induced CHF, the Cx43 in the LA were significantly declined, and there was trend that in both RA and LA, the extent of fibrosis was slightly increased.

Keywords: angiotensin, atrial fibrillation, remodeling, heart failure, statin

Introduction:

Atrial fibrillation (AF) and congestive heart failure (CHF) are two very common cardiovascular disorders, and both are associated with significant morbidity and mortality (1-2). AF eliminates atrial kick for ventricular filling, induces cardiomyopathy, and may worsen the morbidity and mortality of CHF. On the other hand, during CHF, atrial dilatation occurs, which may result in atrial fibrosis or apoptosis, and both structural and electrical remodeling in atria may contribute to the initiation and maintenance of AF (3-7). While antiarrhythmic treatment for AF has been proved to improve CHF (8), non-antiarrhythmic therapy for CHF and ischemic heart disease, such as inhibition of rennin-angiotensin-aldosterone system and anti-inflammation with statins, has recently become another alternative strategy for AF control. However, the underlying mechanisms are not detailed.

In human studies, angiotensin II receptor blocker (ARB) treatment have been shown to be associated with lower AF incidence in CHF patients (9), and statin treatment before cardiac surgery contributes to the reduction of postoperative AF occurrence (10, 11). In animal studies, ARB and statin has been found to attenuate atrial remodeling in canine chronic AF models (12-14). However, their role in CHF mediated atrial remodeling remains unclear.

Non-contact three-dimensional mapping system (EnSite) has been used to improve the mapping and ablation of tachyarrhythmias, especially in complex atrial tachyarrhythmias after surgically corrected congenital heart diseases (15-17). Identification of target sites for ablation is challenging, because reentrant circuits of atrial tachyarrhythmias are complex. The critical sites in these patients are often slow conduction zone (protected isthmus) bordered by scar tissue. EnSite can provide isopotential map with color settings to display the detailed three-dimensional activation mapping for investigating the arrhythmogenic foci or reentrant circuits. In addition, it can also provide global voltage map to define the low voltage zone. Voltage mapping has been developed to allow discrimination of these slow conduction zones from surrounding scar tissues (18). The introduction of three-dimensional mapping systems facilitated the voltage mapping and reconstruction of complex reentrant circuits.

On the other hand, in mammalian heart, there exist gap junctions in specialized plasma membrane regions of atrial cardiomyocytes, and gap junctions in the cardiomyocytes seem to play an important role by forming a direct communicating channel between adjacent cells. Distribution, size, and amount of gap junctions may influence the electrical conduction properties (19,20). Gap junctions in mammalian atrial cardiomyocytes mainly composed of 2 types of connexin (Cx) proteins, Cx 40 and Cx43. In 1994, Saffitz et al showed that the different distribution and characteristics of gap junction Cx protein may determine the different conduction properties presented in atria and ventricles (21). In 2000, van der Velden et al showed that in rapid pacing model, the distribution patterns and the amounts of Cx 40 changed progressively, and the increased Cx 40 distribution heterogeneity correlated with the increased AF stability and structural atrial remodeling (22). Therefore, gap junctional remodeling may play an important role in atrial remodeling and the maintenance of AF. However, the atrial gap junctional remodeling in heart failure remains unclear.

Therefore, the goal of our study in the first year is to evaluate the effects of non-antiarrhythmic treatment with irbesartan and artovastatin on the atrial remodeling (including electrical, structural and gap junctional remodeling) in the canine CHF models.

Methods

Animal preparation

The protocol for animal preparation was approved by the Committee for Experiments on Animals of the Taipei Medical University. Twenty-one mongrel male dogs (weight, 20-30 Kg), 6 control and 6 study dogs, are included. All dogs undergo baseline hemodynamic measurement, then pacemaker implantation and rapid ventricular pacing to result in pacing-induced heart failure, and finally the experimental protocols. The dogs are anesthetized with ketamine (10-20 mg/kg) and sodium pentobarbital (30 mg/Kg intravenous). They are artificially ventilated through a cuffed endotracheal tube by a constant volume cycled respirator with room air. After hemodyamic measurement, a pacing screw-in lead is put in the right ventricular apex through right internal jugular vein. A subcutaneous pocket is fashioned for the placement of a VVI pacemaker (Activitrax or Spectrax, Medtronics). After completing the study, dogs are allowed to recover fully with proper care for 3-7 days. Then, a rapid pacing model is initiated at 240 bpm for 4 to 6 weeks. Pacing-induced heart failure is defined by symptoms of lethargy, loss of appetite, dyspnea and/or ascites. After heart failure develops, the dogs will undergo the following experimental protocols.

Experimental protocols

1. Electrophysiologic study:

Four bipolar hook electrodes are attached to the high right atrium (HRA), low right atrium (LRA), RA appendage (RAA), and left atrial appendage (LAA) to stimulate atrial tissue. One 9 Fr sheath and two 7 Fr sheaths are inserted into right femoral vein, left femoral and right internal jugular vein, respectively. One noncontact mapping balloon catheter is put in RA chamber via the right femoral vein. A quadripolar catheter is inserted via left femoral or right internal jugular vein and used for navigation and contact mapping. Two Spoon high density electrode pads are applied for epicardial contact mapping of RA and LA free walls. Programmed electrical stimulation is performed by a custom-made stimulator (Model 5325, Metronic, Ltd., Minneapolis, USA) that delivered constant-current pulses of 1-ms duration. The atrial effective refractory period (ERP) is determined during atrial pacing (stimulus strength, 2 X threshold) at a cycle length of 300 ms and extrastimulation (S1S2) pacing. S1S2 pacing starts from 300/190 msec and decreases by 10 msec intervals. The shortest S1S2 interval that results in a propagated atrial response is taken as the atrial ERP. The frequency and density of AF occurrence during atrial extrastimulation are calculated by total AF episodes and duration. If AF occurs for more than 5 minutes, DC cardioversion with small paddles (Hewlett Packard, Ltd., Andover, USA) connected to the defibrillator (Codemaster, Hewlett Packard, Ltd., Andover, USA) is given by increasing energy from 2 joules to 5 to 10 joules until sinus rhythm is restored. The dispersions of atrial ERPs are obtained from the differences among these four areas (the maximal minus the minimal ERPs).

2. Noncontact voltage mapping:

After the electrophysiological study, the heart is rapidly removed and placed in cold perfusion fluid. The aorta is cannulated, and the heart is perfused at a pressure of 65 mmHg and a temperature of 37℃. The compositions (in mmol/L) of the perfusion fluid are NaCl 130, NaHCO3 24.2, KCl 4.0, CaCl2 2.2, MgCl2 0.6, Na2HPO4 1.2, and glucose 12. The perfusion fluid is gassed with a mixture of 95% oxygen and 5% CO2, resulting in a pH of 7.4. To maintain the atrial pressure for noncontact mapping, the caval and pulmonary veins are ligated and the perfusion fluid entering the right atrium from the coronary sinus is allowed to leave the heart exclusively through a cannula in the pulmonary artery. The SVC is cannulated with a Y-shaped tube for insertion of noncontact mapping balloon. To balance the pressures of both atria, the interatrial septum is perforated. We have no indication that perforation of the atrial septum affected the vulnerability of the atria for AF. To avoid variation in atrial pressure by contraction of the ventricles, 10 mmol/L butanedione

monoxime (DAM) was given to reduce myocardial contractility.

The noncontact mapping system (EnSite 3000, Endocardial Solutions, Inc., St. Paul, MN, USA) consists of an inflatable multielectrode array (MEA) catheter, a reference electrode, amplifiers, and a Silicon Graphics workstation. Raw data detected by the MEA is fed to the Silicon Graphics workstation via an amplifier. The MEA is positioned in the RA chamber and inflated for mapping. The system locates any catheter in relation to the MEA using a "locator" signal, which is used to construct a three-dimensional computer model of the virtual endocardium, providing a geometry matrix for the inverse solution, and to display and track the position of the catheter on the virtual endocardium. Using mathematical techniques to process the potentials detected by MEA, the system is able to reconstruct more than 3000 unipolar electrograms simultaneously and superimpose them onto the virtual endocardium, producing isopotential maps with a color range representing voltage amplitude. On the isopotential maps, a wave front is defined as a discrete front of endocardial depolarization presenting as a region of negative polarity.

3. Tissue sampling and processing:

After electrophysiological study and noncontact mapping, tissue samples are collected from RAA, RA free wall, crista terminalis, septum, LAA, LA posterior and store in both liquid nitrogen and 10% formalin before cryosectioning and histological examination.

Light microscopy:

Formalin-fixed tissue samples are made into wax blocks, sectioned in 5-μm thickness at room temperature, and stained with Masson's Trichrome for light microscopy.

Immunohistochemistry:

Anti-connexin antibodies and other cell markers

Affinity-purified rabbit polyclonal antisera against Cx40 [designated S15C(R83)] and Cx43 (C16), are used for the immunofluorescence detection of the gap-junctional proteins. Cardiomyocytes are identified with mouse monoclonal antiserum against α-actinin and vinculin (Sigma).

Secondary antibody/detection systems

Donkey anti-rabbit and anti-mouse immunoglobulins conjugated to either CY3, CY5 are used. CY3-conjugated antibodies are used for single labeling and 1 CY3-conjugated plus 1 CY5-conjugated for double labeling. In experiments in which 1 connexin is visualized with the anti-rabit CY3, simultaneous cardiomyocyte marking is detected with the anti-rabit CY5.

I*mmunolabeling of connexins*

For single labeling of one connexin type, cryosections of the samples are blocked in 0.5% BSA (15 minutes) and incubated with rabbit anti-Cx40 (1:200), anti-Cx43 (1:100) at 37℃ for 2 hours. The samples are then treated with CY3-conjugated secondary antibody (1:500, room temperature, 1 hour). When simultaneous marking of cardiomyocytes is carried out, single connexin-labeled samples are incubated with anti-α-actinin (1:200) followed by treatment with the 2 secondary antibodies. Finally, the sections are mounted. All experiments included RA and LA sections as positive controls and omission of primary antibody as negative controls.

Confocal laser scanning microscopy

Immunostained samples are examined by confocal laser scanning microscopy with a Leica TCS SP. The images from sections of multiple labeling are taken with either simultaneous or sequential multiple channel scanning. For determination of the size of and the special relationship between individual cardiomyocytes, in samples labeled with anti-vinculin, consecutive optical sections taken at 0.5-μm intervals through the full thickness of cardiac muscle, in which the long axis of the cells lies horizontal to the sections,

are used. Quantification of gap junction aggregations, defined as the number of aggregations of Cx43-labeled spots in linear or disk shape between the cells, is conducted in samples double-labeled for Cx43 and vinculin by use of similar principles. Quantification is performed with QWIN image analysis software (Leica).

Western blotting

Tissue samples are pulverized in liquid nitrogen and suspended in 3 ml ice-cold lysis buffer. The suspension is incubated on ice and centrifugated, and the soluble fraction is stored at -80˚C. Protein concentration is then determined and protein extracts are denatured in Laemmli buffer and electrophoresed on 10% SDS-polyacrylamide gels. Proteins are transferred to PVDF membranes, blocked with 10% bovine serum albumin (BSA) in Tris-buffered saline (TBS), and incubated overnight in room air or 2 hours in 38˚C in primary antibody solutions.

The following primary antibodies are used for immunodetection: rabbit anti-P44/P42 polyclonal IgG (phosporylated and total ERK), rabbit anti-Cx40 and mouse anti-Cx43. Tissue angiotensin II concentration is measured by ELISA.

Results:

Figure 1 to Figure 4 showed Western blotting analysis of total Cx43 protein levels in the RA of control and CHF dogs. In the RA, the Cx43 levels were similar among normal and CHF dogs. Figure 5 to Figure 8 showed Western blotting analysis of the type I collagen levels in the RA of control and CHF dogs. In the RA, the type I collagen levels were similar among normal and CHF dogs. Figure 9 to Figure 12 showed Western blotting analysis of total Cx43 protein levels in the LA of control and CHF dogs. Except for the LAA, the Cx43 levels were significantly declined in CHF dogs than in normal dogs. Figure 13 to Figure 16 showed Western blotting analysis of type I collagen levels in the LA of control and CHF dogs. In the LA, the type I collagen levels were similar among normal and CHF dogs, indicating that in about 4 to 5 weeks of rapid ventricular pacing for induction of CHF, no significant atrial fibrosis could be found. Although the Cx43 levels in the LA did down-regulated significantly.

Conclusion

In dogs with 4 to 5 weeks of rapid ventricular pacing induced CHF, the Cx43 in the LA were significantly declined, and there was trend that in both RA and LA, the extent of fibrosis was slightly increased.

Reference

1. Wang TJ, Larson MG, Levy D, Vasan RS, Leip EP, Wolf PA, D'Agostino RB, Murabito JM, Kannel WB, Benjamin EJ. Temporal relations of atrial fibrillation and congestive heart failure and their joint influence on mortality: the Framingham Heart Study. Circulation. 2003; 107:2920-5.
2. Gronefeld GC, Hohnloser SH. Heart failure complicated by atrial fibrillation: mechanistic, prognostic, and therapeutic implications. J Cardiovasc Pharmacol Ther. 2003; 8: 107-13.
3. Aime-Sempe C, Folliguet T, Rucker-Martin C, Krajewska M, Krajewska S, Heimburger M, Aubier M, Mercadier JJ, Reed JC, Hatem SN. Myocardial cell death in fibrillating and dilated human right atria. J Am Coll Cardiol. 1999; 34:1577-86.
4. Sanders P, Morton JB, Davidson NC, Spence SJ, Vohra JK, Sparks PB, Kalman JM. Electrical remodeling of the atria in congestive heart failure: electrophysiological and electroanatomic mapping in humans. Circulation. 2003; 108:1461-8.
5. Okuyama Y, Miyauchi Y, Park AM, Hamabe A, Zhou S, Hayashi H, Miyauchi M, Omichi C, Pak

HN, Brodsky LA, Mandel WJ, Fishbein MC, Karagueuzian HS, Chen PS. High resolution mapping of the pulmonary vein and the vein of Marshall during induced atrial fibrillation and atrial tachycardia in a canine model of pacing-induced congestive heart failure. J Am Coll Cardiol. 2003; 42: 348-60.

6. Boixel C, Fontaine V, Rucker-Martin C, Milliez P, Louedec L, Michel JB, Jacob MP, Hatem SN. Fibrosis of the left atria during progression of heart failure is associated with increased matrix metalloproteinases in the rat. J Am Coll Cardiol. 2003; 42: 336-44.
7. Li D, Melnyk P, Feng J, Wang Z, Petrecca K, Shrier A, Nattel S. Effects of experimental heart failure on atrial cellular and ionic electrophysiology. Circulation. 2000; 101: 2631-8.
8. Stevenson WG, Stevenson LW, Middlekauff HR, Fonarow GC, Hamilton MA, Woo MA, Saxon LA, Natterson PD, Steimle A, Walden JA, Tillisch JH. Improving survival for patients with atrial fibrillation and advanced heart failure. J Am Coll Cardiol. 1996;28:1458-1463.
9. Ducharme A, Swedberg K, Pfeffer MA, Cohen-Solal A, Granger CB, Maggioni AP, Michelson EL, McMurray JJ, Olsson L, Rouleau JL, Young JB, Olofsson B, Puu M, Yusuf S; CHARM investigators. Prevention of atrial fibrillation in patients with symptomatic chronic heart failure by candesartan in the candesartan in heart failure: assessment of reduction in mortality and morbidity (CHARM) program. Am Heart J 2006;152:86-92.
10. Ozaydin M, Dogan A, Varol E, Kapan S, Tuzun N, Peker O, Aslan SM, Altinbas A, Ocal A, Ibrisim E. Statin use before by-pass surgery decreases the incidence and shortens the duration of postoperative atrial fibrillation. Cardiology 2006;107:117-121.
11. Patti G, Chello M, Candura D, Pasceri V, D'Ambrosio A, Covino E, DiSciascio G. Randomized trial of atorvastatin for reduction of postoperative atrial fibrillation in patients undergoing cardiac surgery: results of the ARMYDA-3 (Artovastatin for Reduction of Myocardial Dysrhythmia After cardiac surgery) study. Circulation 2006;114:1455-1461.
12. Nakashima H, Kumagai K, Urata H, Gondo N, Ideishi M, Arakawa K. Angiotensin II antagonist prevents electrical remodeling in atrial fibrillation. Circulation 2000;101:2612-2617.
13. Kumagai K, Nakashima H, Urata H, Gondo N, Arakawa K, Saku K. Effects of angiotensin II type 2 receptor antagonist on electrical and structural remodeling in atrial fibrillation. J Am Coll Cardiol 2003;41:2197-2204.
14. Shiroshita-Takeshita A, Schram G, Layoie J, Nattel S. Effect of simvastatin and antioxidant vitamins on atrial fibrillation promotion by atrial-tachycardia remodeling in dogs. Circulation 2004;110:2313-2319.
15. Tai CT, Huang JL, Lin YK, Hsieh MH, Lee PC, Ding YA, Chang MS, Chen SA. Noncontact three-dimensional mapping and ablation of upper loop re-entry originating in the right atrium. J Am Coll Cardiol 2002; 40: 746-753.
16. Liu TY, Tai CT, Lee P C, Hsieh MH, Higa S, Ding YA, Chen SA. Novel concept of atrial tachyarrhythmias originating from the superior vena cava: insight from noncontact mapping. J Cardiovasc Electrophysiol. 2003; 14:533-9.
17. Paul T, Windhagen-Mahnert B, Kriebel T, Bertram H, Kaulitz R, Korte T, Niehaus M, Tebbenjohanns J. Atrial reentrant tachycardia after surgery for congenital heart disease: endocardial mapping and radiofrequency catheter ablation using a novel, noncontact mapping system. Circulation. 2001; 103: 2266-71.
18. de Groot NM, Schalij MJ, Zeppenfeld K, Blom NA, Van der Velde ET, Van der Wall EE. Voltage

and activation mapping: how the recording technique affects the outcome of catheter ablation procedures in patients with congenital heart disease. Circulation. 2003; 108: 2099-106.

19. Davis LM, Kanter HL, Beyer EC, Saffitz JE: Distinct gap junction protein phenotypes in cardiac tissues with disparate conduction properties. J Am Coll Cardiol 1994;24:1124-1132.
20. Davis LM, Rodefeld ME, Green K, Beyer EC, Saffitz JE: Gap junction protein phenotypes of the human heart and conduction system. J Cardiovasc Electrophysiol 1995;6:813-822.
21. Saffitz JE, Kanter HL, Green KG, Tolley TK, Beyer EC: Tissue-specific determinants of anisotropic conduction velocity in canine atrial and ventricular myocardium. Circ Res 1994;74:1065-1070.
22. van der Velden HM, Ausma J, Rook MB, Hellemons AJ, van Veen TA, Allessie MA, Jongsma HJ: Gap junctional remodeling in relation to stabilization of atrial fibrillation in the goat. Cardiovasc Res 2000;46:476-486.

計畫成果自評:

1. **本計畫順利建立心臟衰竭動物模式，並利用三度空間非接觸影像系統於藍根道夫模式下進行動物實驗。**
2. **本年度已成功分析左右心房之間隙連結素在心臟衰竭狗的左心房有遞減的趨勢。**
3. **下一步將同時探討左右心房之病理特徵對治療藥物的反應。**

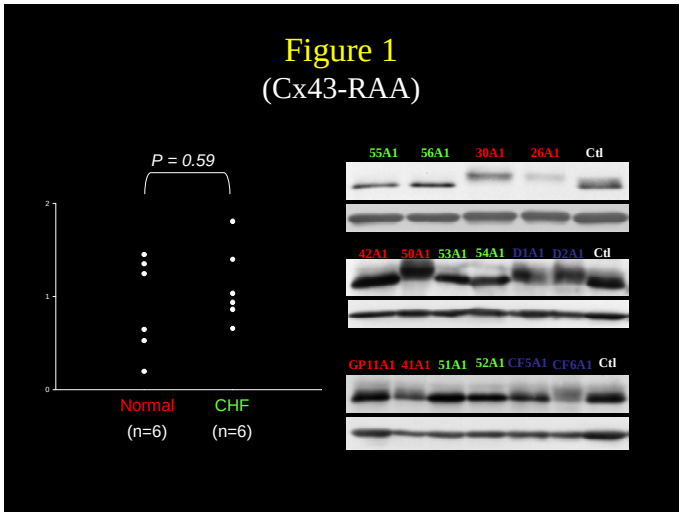

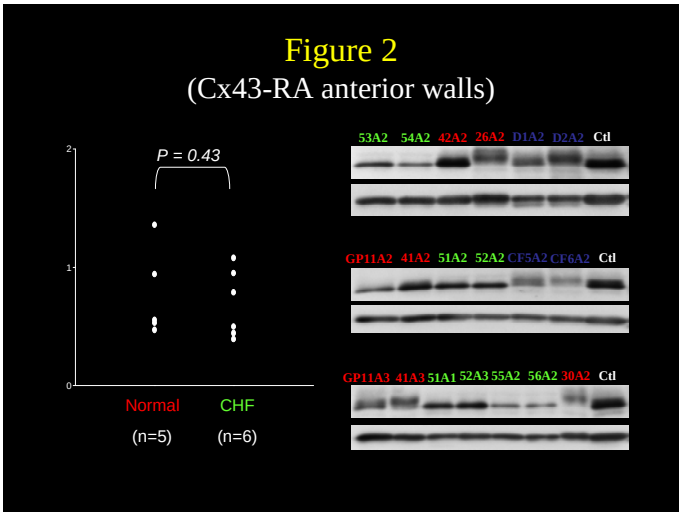

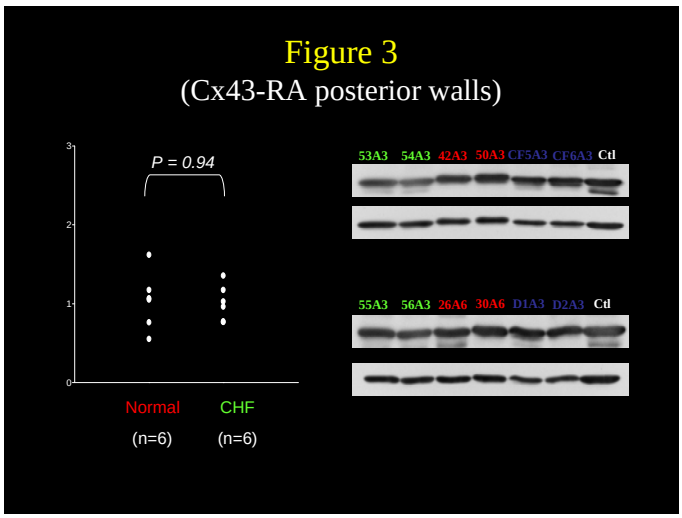

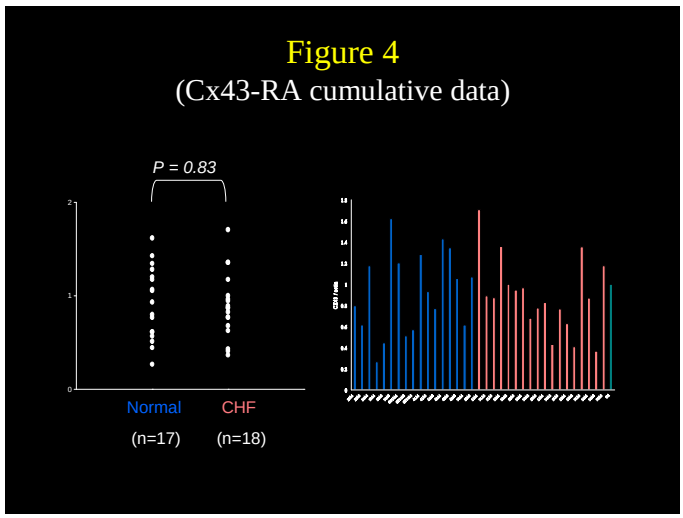

Figure 5
(type 1 Collagen-RAA)

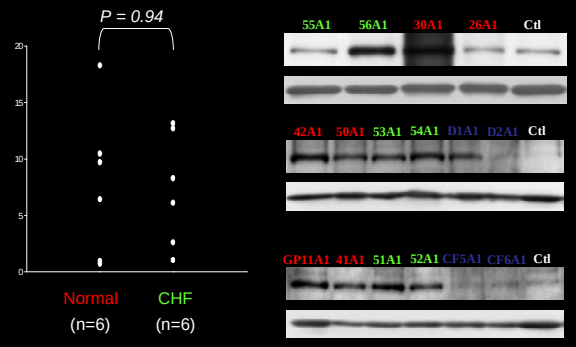

Figure 6
(type 1 Collagen-RA anterior walls)

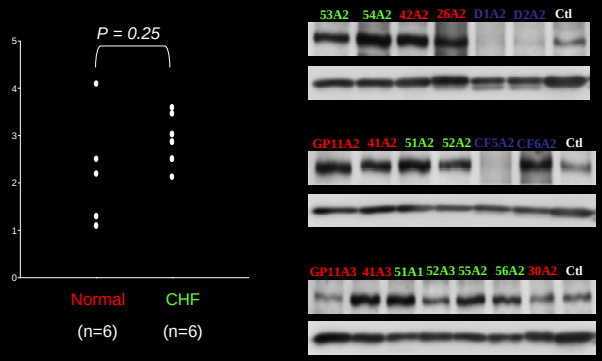

Figure 7
(type 1 Collagen-RA posterior walls)

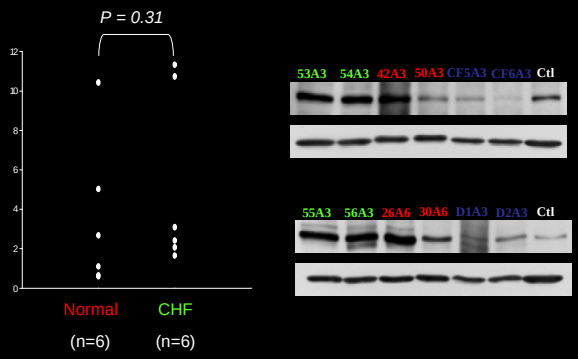

Figure 8
(type 1 Collagen-RA cumulative data)

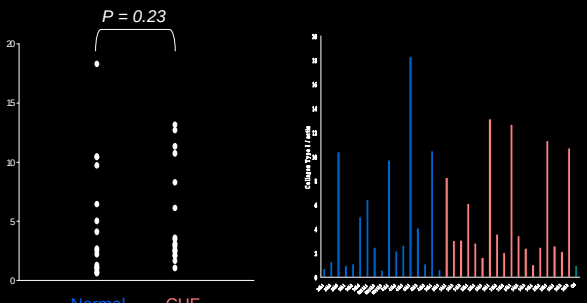

Figure 9
(Cx43-LAA)

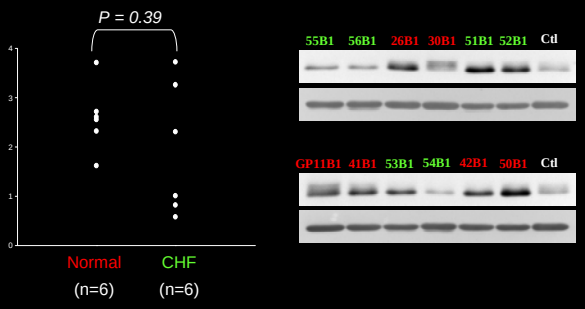

Figure 10
(Cx43-LA anterior walls)

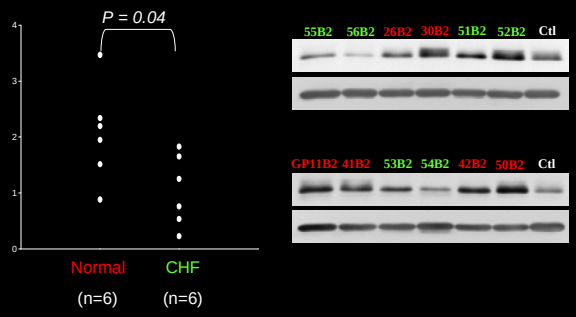

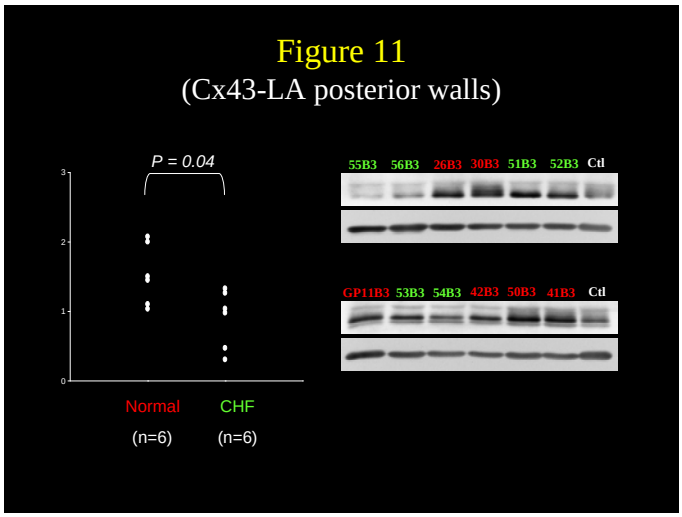

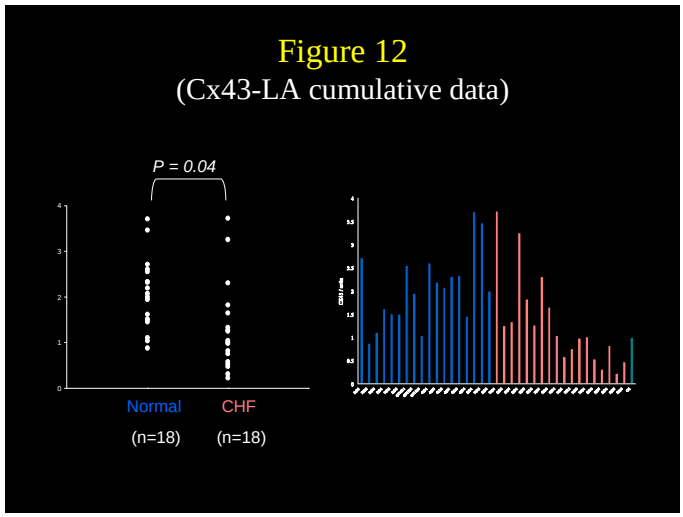

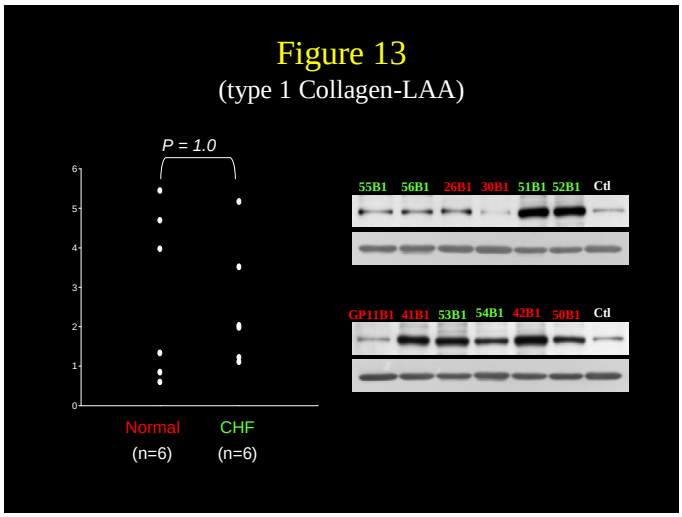

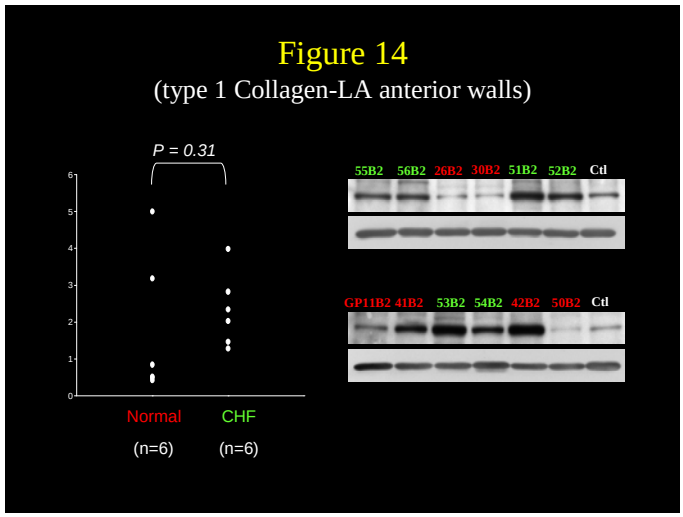

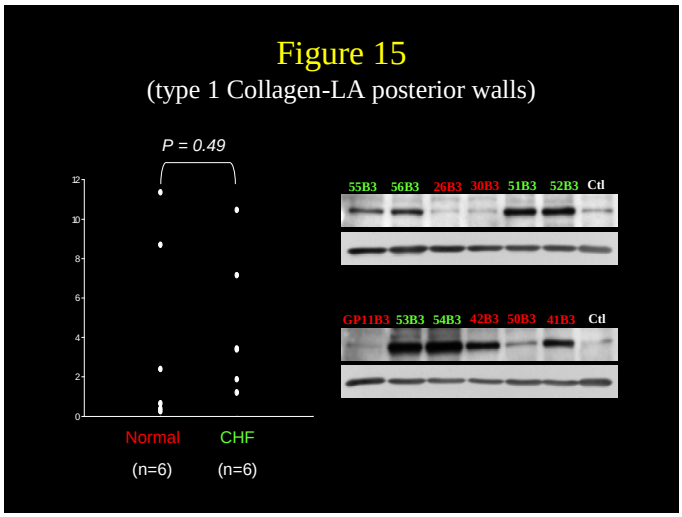

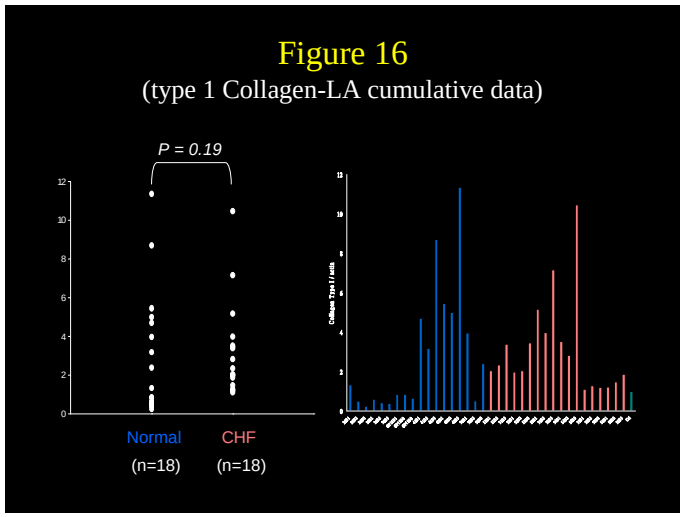

Figure Legends

Figure 1: Western blotting analysis of Cx43 in RAA. Right side showed Cx43 (upper) and actin (lower) bands in Western blotting analysis. Quantitative results were showed in the left side. In RAA, the Cx43 levels were similar between CHF and normal dogs.

Figure 2: Western blotting analysis of Cx43 in RA anterior wall. In RA anterior wall, the Cx43 levels were similar between CHF and normal dogs.

Figure 3: Western blotting analysis of Cx43 in RA posterior wall. In RA posterior wall, the Cx43 levels were similar between CHF and normal dogs.

Figure 4: Cumulative Western blotting analysis of Cx43 in RA. In RA, the Cx43 levels were similar between CHF and normal dogs.

Figure 5: Western blotting analysis of type I collagen levels in RAA. Right side showed type I collagen (upper) and actin (lower) bands in Western blotting analysis. Quantitative results were showed in the left side. In RAA, the type I collagen levels were similar between CHF and normal dogs.

Figure 6: Western blotting analysis of type I collagen levels in RA anterior wall. In RA anterior wall, the type I collagen levels were similar between CHF and normal dogs.

Figure 7: Western blotting analysis of type I collagen levels in RA posterior wall. In RA posterior wall, the type I collagen levels were similar between CHF and normal dogs.

Figure 8: Cumulative Western blotting analysis of type I collagen levels in RA. In RA, the type I collagen levels were similar between CHF and normal dogs.

Figure 9: Western blotting analysis of Cx43 in LAA. Right side showed Cx43 (upper) and actin (lower) bands in Western blotting analysis. Quantitative results were showed in the left side. In LAA, the Cx43 levels were similar between CHF and normal dogs.

Figure 10: Western blotting analysis of Cx43 in LA anterior wall. In LA anterior wall, the Cx43 were declined in CHF dogs, as compared with normal dogs.

Figure 11: Western blotting analysis of Cx43 in LA posterior wall. In LA posterior wall, the Cx43 were declined in CHF dogs, as compared with normal dogs.

Figure 12: Cumulative Western blotting analysis of Cx43 in LA. In LA, the Cx43 were declined in CHF dogs, as compared with normal dogs.

Figure 13: Western blotting analysis of type I collagen levels in LAA. Right side showed type I collagen (upper) and actin (lower) bands in Western blotting analysis. Quantitative results were showed in the left side. In LAA, the type I collagen levels were similar between CHF and normal dogs.

Figure 14: Western blotting analysis of type I collagen levels in LA anterior wall. In LA anterior wall, the type I collagen levels were increased in CHF dogs, as compared with normal dogs.

Figure 15: Western blotting analysis of type I collagen levels in LA posterior wall. In LA posterior wall, the type I collagen levels were similar between CHF and normal dogs.

Figure 16: Cumulative Western blotting analysis of type I collagen levels in LA. In LA, the type I collagen levels were similar between CHF and normal dogs, although there were trends that in CHF dogs, the fibrosis tended to be more prominent.